Journal of Semiconductors
(2019) 40, 081503
doi: 10.1088/1674-4926/40/8/081503

REVIEWS

# Interlayer exchange coupling in (Ga,Mn)As ferromagnetic semiconductor multilayer systems

**Sanghoon Lee[1, †], Sunjae Chung[1], Hakjoon Lee[1], Xinyu Liu[2], M. Dobrowolska[2], and J. K. Furdyna[2]**

[1]Department of Physics, Korea University, Seoul 136-701, Korea

[2]Department of Physics, University of Notre Dame, Notre Dame, Indiana 46556, USA

**Abstract:** This paper describes interlayer exchange coupling (IEC) phenomena in ferromagnetic multilayer structures, focusing on the unique IEC features observed in ferromagnetic semiconductor (Ga,Mn)As-based systems. The dependence of IEC on the structural parameters, such as non-magnetic spacer thickness, number of magnetic layers, and carrier density in the systems has been investigated by using magnetotransport measurements. The samples in the series show both a typical anisotropic magnetoresistance (AMR) and giant magnetoresistance (GMR)-like effects indicating realization of both ferromagnetic (FM) and antiferromagnetic (AFM) IEC in (Ga,Mn)As-based multilayer structures. The results revealed that the presence of carriers in the nonmagnetic spacer is an important factor to realize AFM IEC in this system. The studies further reveal that the IEC occurs over a much longer distance than predicted by current theories, strongly suggesting that the IEC in (Ga,Mn)As-based multilayers is a long-range interaction. Due to the long-range nature of IEC in the (Ga,Mn)As-based systems, the next nearest neighbor (NNN) IEC cannot be ignored and results in multi-step transitions during magnetization reversal that correspond to diverse spin configurations in the system. The strength of NNN IEC was experimentally determined by measuring minor loops that correspond to magnetization flips in specific (Ga,Mn)As layer in the multilayer system.

**Key words:** thin film; crystal; ferromagnetic semiconductor; interlayer coupling

**Citation:** S Lee, S Chung, H Lee, X Y Liu, M Dobrowolska, and J K Furdyna, Interlayer exchange coupling in (Ga,Mn)As ferromagnetic semiconductor multilayer systems[J]. *J. Semicond.*, 2019, 40(8), 081503. http://doi.org/10.1088/1674-4926/40/8/081503

## 1. Introduction

Interlayer exchange coupling (IEC) in magnetic multilayers is a spin interaction that determines spontaneous alignment of magnetization between magnetic layers. The magnetization alignment, either parallel or anti-parallel, between two adjacent ferromagnetic layers causes different scattering of charge carriers. The magnitude of electric current passing through a magnetic multilayer structure is then modulated by the relative orientation of magnetization vectors between ferromagnetic layers reaching its maximum for parallel and minimum for antiparallel configuration. Such dependence of resistance on the spin configurations in turn leads to the phenomenon known as giant magnetoresistance (GMR), that was first observed in the Fe/Cr/Fe trilayer[1] and Fe/Cr multilayer[2] structures. Since the discovery of the GMR effect, it has been serving as a key ingredient in electrically controlled magnetic memory and sensor devices, as well as high-density read-head technology[3]. The detailed understanding of the nature of IEC between magnetic layers becomes essential for the utilization of the magnetic multilayer structure in spintronic devices.

The properties of IEC in metallic ferromagnetic (FM) multilayers have already been extensively investigated in this context, and the ability to control the IEC by structural parameters to be either FM or antiferromagnetic (AFM) is now well established[4–7]. Such extensive investigation of IEC in metallic multilayers led to the realization of new spin based electronic devices, including magnetic random access memory (MRAM) – a practical spin memory device. Even though the metallic ferromagnetic multilayers have provided the core structures of magnetic memory devices, the manipulation of magnetization is limited to use in the current induced effective magnetic field, which still requires the relatively large current density of ~$10^6$–$10^7$ A/cm$^2$[8–10]. It is, therefore, desirable to have other ferromagnetic multilayer systems, in which the magnetizations and relative configurations can be more effectively controlled by various means.

A magnetic multilayer based on (Ga,Mn)As ferromagnetic semiconductor is an interesting material system, since the magnetic properties of the (Ga,Mn)As can be controlled by numerous external means, such as gate voltage, magnetic field, strain, and light illumination[11–15]. Such versatile controllability of magnetic properties in (Ga,Mn)As will provide a significant advantage in designing spintronic devices involving (Ga,Mn)As layers. For example, the IEC in (Ga,Mn)As-based multilayers can be controlled not only by changing spacer thickness but also by tuning the energy barrier of spacer and carrier density in the system. This will provide a new handle for the manipulation of magnetic alignment, thus the resistance in the multilayer system.

In this paper, we review the IEC phenomena of (Ga,Mn)As-based multilayers investigated by magneto-transport experiments. We have concentrated on describing the spontaneous realization of both antiferromagnetic (AFM) and ferromagnetic (FM) spin alignment between ferromagnetic (Ga,Mn)As lay-

Correspondence to: S Lee, slee3@korea.ac.kr
Received 22 MAY 2019; Revised 3 JUNE 2019.
©2019 Chinese Institute of Electronics

Table 1. Description of parameters and structures for the sample series from A to E. (Adapted from Ref. [16])

| Sample | # of (Ga,Mn)As layers | Spacer layer | (Ga,Mn)As thickness $d_m$ (nm) | Spacer layer thickness $d_{nm}$ (nm) | Mn composition (%) | Carrier concentration $p$ (cm$^{-3}$) | IEC type |
|---|---|---|---|---|---|---|---|
| A1 | 10 | GaAs | 6.9 | 0.7 | 3 | $1.0 \times 10^{20}$ | FM |
| A2 | 10 | GaAs | 6.9 | 2.3 | 3 | $8.9 \times 10^{19}$ | FM |
| A3 | 10 | GaAs | 6.9 | 3.5 | 3 | $7.8 \times 10^{19}$ | FM |
| A4 | 10 | GaAs | 6.9 | 7.1 | 3 | $5.8 \times 10^{19}$ | FM |
| B1 | 10 | GaAs:Be | 6.9 | 1.2 | 3 | $1.2 \times 10^{20}$ | FM |
| B2 | 10 | GaAs:Be | 6.9 | 2.3 | 3 | $1.2 \times 10^{20}$ | FM |
| B3 | 10 | GaAs:Be | 6.9 | 3.5 | 3 | $1.2 \times 10^{20}$ | AFM |
| B4 | 10 | GaAs:Be | 6.9 | 7.1 | 3 | $1.2 \times 10^{20}$ | AFM |
| C1 | 2 | GaAs:Be | 17.2, 8.6 | 4.3 | 5 | $1.4 \times 10^{19}$ | FM |
| C2 | 2 | GaAs:Be | 17.2, 8.6 | 4.3 | 5 | $1.0 \times 10^{20}$ | FM |
| C3 | 2 | GaAs:Be | 17.2, 8.6 | 4.3 | 5 | $2.0 \times 10^{20}$ | AFM |
| D1 | 6 | GaAs:Be | 8.5 | 4.2 | 1.2 | $2.0 \times 10^{19}$ | FM |
| D2 | 6 | GaAs:Be | 8.5 | 4.2 | 1.2 | $1.9 \times 10^{20}$ | AFM |
| E2 | 8 | GaAs:Be | 8 | 4 | 3.5 | $1.1 \times 10^{20}$ | AFM |
| E3 | 8 | GaAs:Be | 8 | 4 | 6.5 | $1.5 \times 10^{19}$ | FM |
| E4 | 9 | GaAs:Be | 8 | 4 | 6.5 | $1.4 \times 10^{19}$ | FM |

ers, which in turn strongly depends on the structural parameters such as non-magnetic spacer thickness and carrier density in the systems. We have also noticed that the IEC in the (Ga,Mn)As-based multilayers is a long-range interaction reaching tens of nanometers. The IEC in the (Ga,Mn)As multilayers can reach the next nearest neighbor (NNN) interaction, which significantly affects magnetization reversal of the systems by showing multi-step transitions correspond to various spin configurations of the structures.

## 2. Experiment

All (Ga,Mn)As-based multilayer samples were grown by molecular beam epitaxy (MBE) on (001) GaAs substrates. Several series of (Ga,Mn)As-based multilayer structures were designed by varying structural parameters of the multilayers, such as non-magnetic spacer thickness, carrier density, Mn concentration in the (Ga,Mn)As layer, and number of repetitions of the multilayer structures. These sets of samples are referred to as series A through E. Detailed descriptions of the sample structures are given in Table 1[16]. The structural properties, such as chemical composition of the (Ga,Mn)As and the thicknesses of the layers, were investigated by using X-ray diffraction measurement. Magnetization of the samples was measured using a quantum design superconductor quantum interference device (SQUID) magnetometer.

For the transport measurements, a Hall device with the long dimension along the [110] (or [1-10]) direction was patterned on the specimen by photolithography and dry (or chemical) etching. The Hall device has six probes and the width of the current channel ranges from 10–300 $\mu$m depending on the sample. Magnetotransport measurements were carried out in a closed cycle cryostat using a cold finger whose temperature can be varied from 3 to 300 K. The PHR measurements were performed using a sample holder designed so as to allow a magnetic field to be applied in arbitrary directions in the plane of the sample. The temperature dependence of resistance in the absence of magnetic field shows resistance peaks, which provides an estimation of Curie temperatures for the (Ga,Mn)As layers[17–19]. The carrier concentrations of the samples were estimated from Hall measurements at room temperature and are listed in Table 1. The carrier concentrations of the GaAs:Be spacer was estimated from a reference epilayer, which was grown at the same growth condition as in the GaAs:Be spacer. It has ~$1.2 \times 10^{20}$ cm$^{-3}$ which is close to the average carrier concentration of multilayer samples.

## 3. Magnetotransport of the (Ga,Mn)As-based multilayers

### 3.1. Observation of FM and AFM interlayer exchange coupling

In order to investigate the IEC between (Ga,Mn)As layers, we used magnetoresistance (MR) measurements, which show different values depending on the alignment of magnetization between magnetic layers. We first studied the sample series A and B, which are $[(Ga,Mn)As/GaAs]_{10}$ and $[(Ga,Mn)As/GaAs:Be]_{10}$ structure (i.e., the two series are nearly the same except Be in the GaAs spacer). The thickness of the non-magnetic GaAs spacer was systematically varied from 0.7–7.1 nm within each series. These two series of samples were designed to address the dependence of IEC on the spacer thickness and on the carrier density of the (Ga,Mn)As multilayers. Measurements were performed at 30 K with current along the [1-10] direction (i.e., long dimension of the Hall device for sample series A and B) and the external field applied near the [110] crystallographic direction. The temperature of 30 K was selected in order to maximize IEC effect during the magnetization reversal process, which was dominated by crystalline anisotropy at low temperature[20–23]. The MR data are plotted in Fig. 1, where the first and the second columns show data from series A and B, respectively. The data in the first column show positive MR over a wide range of applied fields, with two reversed horn-like features at low fields in the magnetization reversal process. This is a typical anisotropic magnetoresistance (AMR) of a single layer (Ga,Mn)As film, which is determined by the angle between the magnetization vector and the direction of the current[24, 25]. The observed single layer behavior in the $[(Ga,Mn)As/GaAs]_{10}$ multilayers indicates that the IEC between the ferromagnetic

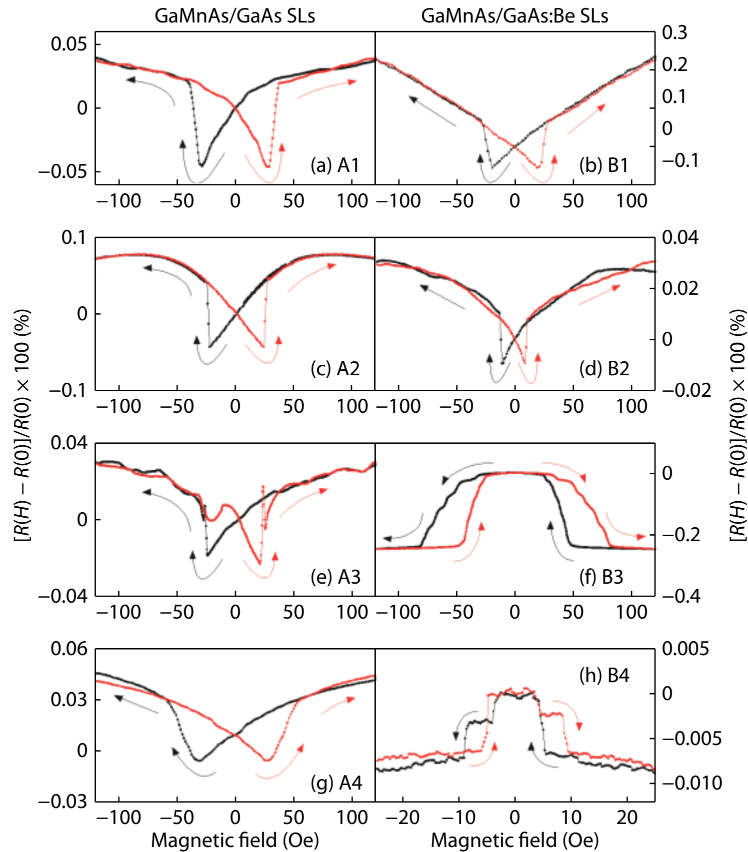


Fig. 1. (Color online) Magnetoresistance of (Ga,Mn)As/GaAs multilayers measured with magnetic field applied near the [110] direction at $T = 30$ K. Although the AMR typical for (Ga,Mn)As layers dominates the MR observed in most of the samples, giant magnetorsistance (GMR)-like effect is clearly seen in samples B3 and B4, indicating the presence of AFM IEC in those specimens. The arrows indicate the direction of field scan. (Adapted from Ref. [20])

(Ga,Mn)As layers in series A is most likely FM.

In contrast, the MR data obtained from series B shows quite different behavior during the magnetization reversal process. While the B1 and B2 samples with thin GaAs:Be spacer (i.e, 1.2 and 2.3 nm) show typical AMR of a single layer (Ga,Mn)As film (see top two panels in the right column of Fig. 1), other two samples (B3 and B4) clearly show that the lowest resistance occurs at saturated states with large field, and the highest resistance occurs at zero field. Since the parallel and antiparallel alignments give small and large resistance, respectively, in the magnetic multilayer, the magnetization of (Ga,Mn)As layers are parallel in large fields and antiparallel at zero field. Such spontaneous alignment of antiparallel configuration between (Ga,Mn)As layers at zero field clearly indicates the presence of AFM IEC in these two samples. Specially, as the field strength is reduced in returning sweep, the resistance value returns to maximum even before the field direction is reversed. This is because the magnetization alignment between successive (Ga,Mn)As magnetic layers is recovered to antiparallel by AFM IEC with reducing field strength. The investigation of series A and B reveals that the presence of carrier in the GaAs spacer layer is critical for the realization of AFM IEC between (Ga,Mn)As layers and types of IEC can be changed between FM and AFM by varying spacer thickness.

The IEC investigation was further extended to diverse multilayer structures with different structural parameters listed as series C–E in Table 1. In those series, however, the non-magnetic spacer layer was always doped with Be to increase the possibility of observing AFM IEC, which was shown only in Be doped samples in the results of series A and B as described above. For these samples, the Hall device was patterned with long direction (i.e, current direction) along the [110] direction. The MR measurements were performed with the external field along the [110] crystallographic direction. The MR data taken from six representative samples (two samples from each series C, D, and E) are plotted in Fig. 2, where the panels in the first and the second rows show data obtained at 3 and 30 K, respectively. All the data in the first row shows typical AMR behavior of single layers of (Ga,Mn)As grown on GaAs substrates as already discussed above. This is because magnetic anisotropy of (Ga,Mn)As layer at low temperature is very strong and it dominates the magnetization reversal process. In contrast, when temperature increases to 30 K, the magnetic anisotropy of (Ga,Mn)As layer significantly decreases[26] and the IEC between the (Ga,Mn)As layers can affect the magnetization reversal process. Samples C1, D1, and E2 show AMR similar to the single (Ga,Mn)As layer even at 30 K, indicating the presence of FM IEC in these samples. However, samples C3, D2, and E3 clearly show a maximum resistance at zero field during the field scans. Such recovery of the resistance maximum at zero field during field cycling is typically observed in magnetic multilayer systems with AFM IEC[20, 22, 23], and represents the mechanism responsible for giant magnetoresistance (GMR). The observation of this GMR-like effect in these (Ga,Mn)As-based multilayers with different structural parameters provides additional evidence that the AFM IEC such as that discussed in the previ-

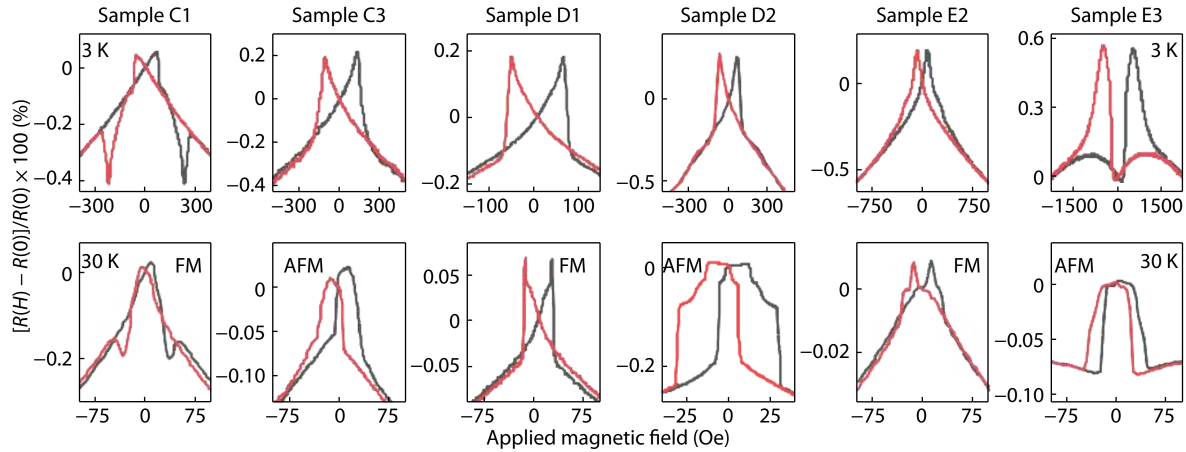


Fig. 2. (Color online) Magnetoreistance observed in six (Ga,Mn)As/GaAs multilayers with different structural parameters. Samples C1, D1, and E2 show only anisotropic magnetoresistance (AMR), characteristic of FM IEC between the (Ga,Mn)As layers; Samples C3, D2, and E3 show a GMR-like behavior, indicating the presence of AFM IEC in these samples similar to that seen in the $[(Ga,Mn)As/GaAs:Be]_{10}$ multilayer discussed in detail in the Fig. 1.

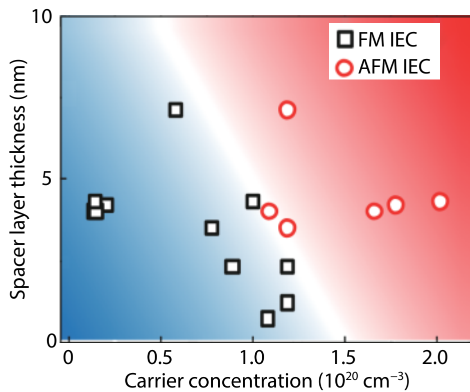


Fig. 3. (Color online) Summary plot of IEC type for the various (Ga,Mn)As multilayers depending on carrier concentrations and spacer layer thicknesses. Black open squares and red open circles show FM IEC and AFM IEC, respectively. (Adapted from Ref. [16])

ous paragraph (i.e., regarding sample B3 and B4) is a general characteristic and can be reproducibly realized by appropriate selection of structural parameters.

In order to see the dependence of the IEC on the structure parameters, we have generated plots summarizing the results of all samples. Fig. 3 shows the plot of non-magnetic spacer thickness (vertical axis) versus carrier concentration (horizontal axis) for the multilayer sample. The open red circles and open black squares correspond to the samples showing AFM and FM IEC, respectively. Note that the two symbols are positioned in two isolated regions marked with red and blue backgrounds in Fig. 3. The red circles representing the samples with AFM IEC appear only in the isolated region bounded by the carrier concentration of $1.00 \times 10^{20}$ cm$^{-3}$ and by the spacer thickness of 3.5 nm. However, the samples showing FM IEC (i.e., presented with black squares) spread out over a wide range of spacer thickness when the carrier concentration is below $1.25 \times 10^{20}$ cm$^{-3}$. This behavior indicates that the carrier concentration as well as spacer thickness are crucial parameters for the realization of AFM IEC in (Ga,Mn)As multilayers.

Note further that the spacers in our AFM IEC samples are as thick as 7 nm (i.e., sample B4), which is much greater than those typically used for ferromagnetic metal-based multilayer systems[2, 27] and those predicted by theory[28–30]. One may ascribe this to the properties of the Fermi wavelength, which is the fundamental factor for defining the interaction range of the mediating carriers. The Fermi wave vectors is given by $k_{\rm F} = (3\pi^2 n)^{1/3}$, where $n$ is the carrier concentration. The carrier concentration of ferromagnetic (Ga,Mn)As is typically of the order of a few $10^{20}$ cm$^{-3}$, which is several orders of magnitude smaller than the carrier concentration in intrinsic metals. This should lead to much longer Fermi wave lengths, $\lambda_{\rm F} \sim 4$ nm, in ferromagnetic semiconductors than in metallic ferromagnets. Therefore, the IEC in magnetic multilayers consisting of ferromagnetic semiconductors such as (Ga,Mn)As can have a much longer distance. Such long-range nature of IEC in (Ga,Mn)As-based multilayers significantly affects the magnetization reversal process as will be discussed in the next section.

### 3.2. Observation next-nearest-neighbor (NNN) IEC between (Ga,Mn)As layers

Magnetization reversal of magnetic multilayers, in which magnetic layers are coupled to each other, can be strongly affected by exchange coupling. Even though the nature of IEC has been intensively studied in systems involving various ferromagnetic (FM) materials[4, 5, 23, 31–35], the understanding of mechanisms leading to IEC – such as the dependence of the interlayer coupling strength on structural parameters and the oscillation of IEC between FM and AFM[6, 7] in such multiple layer structures – has so far been based only on nearest-neighbor (NN) interactions in magnetic multilayer structures[28–30]. In particular, in discussing IEC-related effects of multilayer structures consisting of more than two magnetic layers, the effects arising from higher-order IEC has been totally ignored. The IEC strength in a magnetic multilayer, estimated from the Ruderman–Kittel–Kasuya–Yosida (RKKY)-type carrier-mediated spin-spin interaction, decreases as $1/r^2$, where $r$ is the cumulative non-magnetic distance separating the magnetic layers[36–38]. Since in a [magnetic/non-magnetic]$_n$ multilayer system the total thickness of non-magnetic layers between next-nearest magnetic layers is twice the distance between the nearest-neighbor magnetic layers, according to this picture one can expect the NNN coupling strength to be 1/4 of the NN coupling. This estimated magnitude of NNN IEC is not sufficiently small to be ignored in dis-

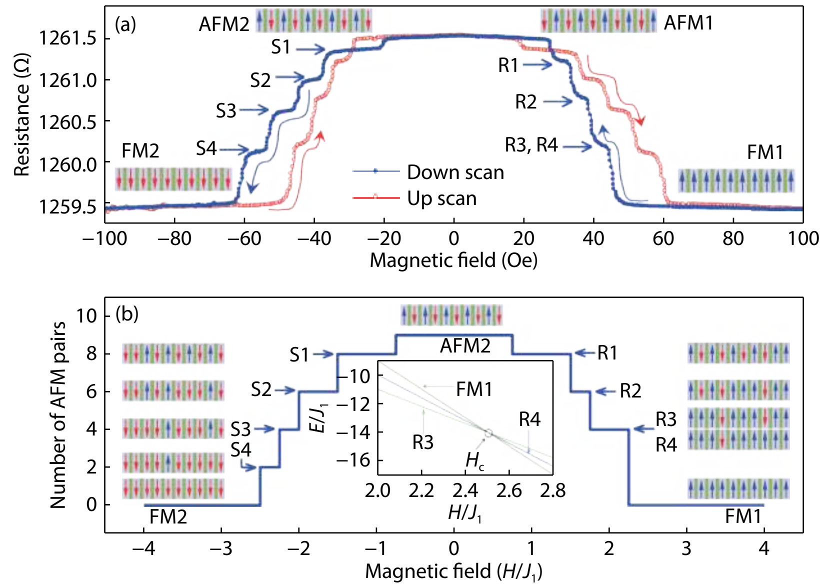


Fig. 4. (Color online) The process of magnetization reversal in the [(Ga,Mn)As/GaAs:Be]10 multilayer system. (a) MR is measured at 35 K as the field is cycled between −100 and 100 Oe. The down- and up-scans, shown by solid (blue) and open (red) circles, respectively, have a completely symmetrical behavior. Two types of fully AFM spin configurations between the (Ga,Mn)As layers, AFM1 and AFM2, can be realized at zero field, as shown schematically by the vertical arrows. Each field scan (down or up) contains a four-step restoring process and a five- step saturation process, with resistance plateaus marked as R1–R4 and S1–S4. (b) The number of pairs with AFM alignment between adjacent (Ga,Mn)As layers in the multilayer is obtained by minimizing the IEC energy given by Eq. (1) during the down-scan of the field. The field is scaled in terms of the NN IEC strength $J_1$. The reversal process determined from calculation using Eq. (1) clearly shows a four-step restoring and a five-step saturation process, similar to that observed in the MR experiment shown in the upper panel. The crossing of the calculated energies for the R3, R4 and FM1 states is shown in the inset. The spin configuration corresponding to each plateau in the field scan is indicated schematically by vertical arrows. (Adapted from Ref. [40])

cussing IEC-related effects.

The (Ga,Mn)As-based multilayers has special implications in investigating the effects arising from higher-order IEC due to the long-range nature of IEC as mentioned in the previous section. The IEC can reach other (Ga,Mn)As layers over the NN in multilayer structures consisting of more than two magnetic layers. The magnetization reversal process of such multilayers will be significantly modified and will be more complicated by the influence of NNN IEC. Here, we focus on the sample B4 (i.e., $[(Ga,Mn)As/GaAs:Be]_{10}$ structure that was shown in the third panel of the second column in Fig. 1) in order to show the effect of NNN IEC in the magnetization reversal of (Ga,Mn)As-based multilayers.

Fig. 4(a) shows MR data obtained during magnetization reversal with the applied magnetic field oriented near the [110] direction at 35 K. The data show many transition steps in the saturation (i.e, increasing the field in either direction, which eventually aligns the magnetization of all (Ga,Mn)As layers parallel) and the restoring sweeps (i.e, reducing the field to zero) marked as S1–S4 and R1–R4, respectively. This implies that the magnetizations of those (Ga,Mn)As layers reverse independently as the field increases or decreases in the reversal process.

In magnetic multilayer system with strong AFM IEC, the magnetic layers form two types of anti-parallel spin configurations, AFM1 (↓↑ ··· ↓↑) or AFM2 (↑↓ ··· ↑↓), as schematically shown in Fig. 4(a) for $H = 0$, in which arrows indicate the directions of magnetization. The outermost layers (i.e, the bottom and the top layers) have only one nearest magnetic layer, while all other magnetic layers inside the structure have two magnetic nearest neighbors that can interact antiferromagnetically with that inner layer. Thus, the AFM IEC in the case of the two outermost layers is roughly half as strong as in the case of magnetic layers located inside the system when we consider only NN IEC in the system. This will then result in a two-step transition of magnetization as it is taken to saturation by the applied field (or restored by reducing the magnetic field to zero), regardless of the number of magnetic layers comprising the multilayer structure[4, 39]. In our $[(Ga,Mn)As/GaAs:Be]_{10}$ SL it is obvious that the first transition in the saturation process corresponds to the flip of magnetization in one of the outermost (Ga,Mn)As layers (i.e., either the bottom or the top (Ga,Mn)As layer, depending on which of those is magnetized antiparallel to the applied field). It is obvious that the multiple steps seen in the magnetoresistance in Fig. 4(a) must correspond to different internal layers flipping their magnetizations at different fields. However, it is impossible to understand the multiple steps of transitions by considering the NN IEC alone. The phenomenon must involve additional interaction terms that differentiate the strengths of IEC acting on specific interior (Ga,Mn)As layers. The most likely interaction for removing the energy degeneracy of magnetization alignments of the interior (Ga,Mn)As layers determined by NN AFM IEC is the NNN IEC.

The interlayer exchange coupling energy $E$ of the our $[(Ga,Mn)As/GaAs:Be]_{10}$ SL in the presence of a magnetic field $H$ by including NNN IEC contributions can be expressed in the form[40]

$$E = \sum_{i=1}^{9} J_1(M_i M_{i+1}) + \sum_{i=1}^{8} J_2(M_i M_{i+2}) - \sum_{i=1}^{10} HM_i, \qquad (1)$$

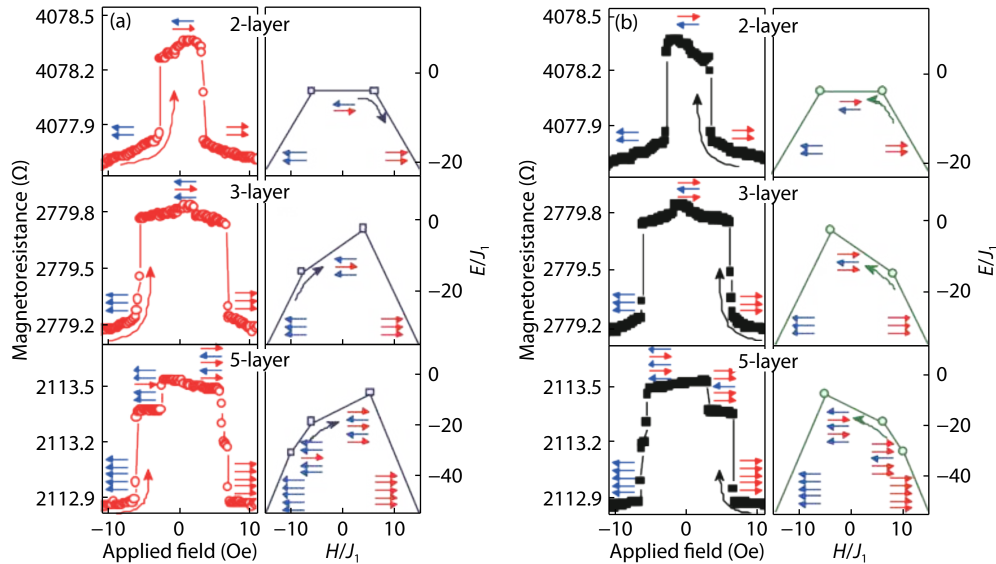


Fig. 5. (Color online) Magnetic field dependence of MR and IEC energy during (a) up-scan and (b) down-scan of applied field for samples used in this study. The experimentally measured MR at 23 K and calculated IEC energy for possible spin configurations are plotted in left and right columns of each figure, respectively. (Adapted from Ref. [43])

where $J_1$ and $J_2$ are the NN and NNN IEC constants, respectively, and $M_i$ is the magnetization of the $i$th magnetic layer. The magnetic field dependence of the IEC energy for various spin configurations without NNN IEC contribution in Eq. (1) only explains two step-transitions (i.e., first the outermost magnetic layer and all interior magnetic layers initially aligned opposite to the field) in both the saturation and the restoring processes[40].

However, when the strength of NNN IEC, $J_2 = 0.25J_1$, is included in the calculation, the energy dependences of spin configurations are altered and many possible transitions appear in the restoring and saturation process. The magnetization reversal path obtained by calculating the lowest coupling energy for the down-scan case is shown in Fig. 4(b), which reproduces the observed four-step restoration and the five-step saturation processes. The spin configurations during down-scan are schematically shown in the Fig. 4(b). The detailed calculation and identification of spin configurations correspond to transitions are given in Ref. [40]. Interestingly, R4 and R3 states have the same energy at $H_c$ (see inset of Fig. 4(b)) resulting in the four-step restoration.

Since the transition fields are all different for the (Ga,Mn)As layers in the multilayer system, the magnitude of the total IEC acting on each (Ga,Mn)As layer can be different. The magnitude of the IEC acting on each magnetic layer in $[(Ga,Mn)As/GaAs:Be]_{10}$ multilayer was investigated by Chung *et al.*[21], using a series of partial (minor) hysteresis loop experiments, in which magnetization reversal occurs only in specific (Ga,Mn)As layers, and not in others. The magnitudes of NN IEC for all (Ga,Mn)As layers obtained in that study lie in the range of 20 to 30 Oe, with the exception of the top (Ga,Mn)As layer, which is about twice as large as the values for the other (Ga,Mn)As layers. The result indicates that all inner (Ga,Mn)As layers experience similar NN IEC. The unexpectedly large coupling strength for the top magnetic layer may be due to the difference of magnetic properties of top (Ga,Mn)As, that has unintentional out-diffusion of Mn during growth and exposed Mn on the surface[41, 42].

### 3.3. Quantitative determination of NNN IEC between (Ga,Mn)As layers

The multi-step transitions that are observed from (Ga,Mn)As multilayers can be understood based on the sequence of spin alignments between the (Ga,Mn)As layers which is experienced during magnetization reversal. In order to describe this effect theoretically, the strength of NNN IEC was taken to be one quarter of the NN IEC considering the geometry of the multilayer[36–38]. The strengths of NNN IEC relative to the NN IEC assumed from theory can be addressed by studying multilayers, which have different numbers of NN and NNN (Ga,Mn)As layers[43]. The MR was measured at 23 K on the three multilayers with two, three, and five (Ga,Mn)As layers and is plotted in Fig. 5. The data obtained during the field up-scan and down-scan are plotted in the left columns of Figs. 5(a) and 5(b), respectively. The GMR-like effect is seen in all data indicating the presence of AFM IEC between (Ga,Mn)As layers in all multilayer structures. The step-like MR “jumps” can be described by the dependence of the IEC energy on the field, which can be calculated from Eq. (1). The right columns of Figs. 5(a) and 5(b) show the spin configurations that correspond to the lowest IEC energy during the up-scan and down-scan, respectively.

The minor hysteresis loop formed by magnetization reversal of only one specific (Ga,Mn)As layer provides the information on the IEC field felt by a given (Ga,Mn)As layer. Fig. 6 shows such minor loops obtained from the negative field region (i.e, minor loop of MR data shown in Fig. 5(a)) for all three structures. The arrows in Fig. 6 show the initial and final spin alignments for each minor loop. As can be seen from the spin configurations, only one (Ga,Mn)As layer experiences magnetization reversal during minor loop scans. The shift of hysteresis, therefore, is proportional to the total IEC strength felt by that specific (Ga,Mn)As layers. The (Ga,Mn)As layer experiencing the magnetization reversal in minor scan has one NN for the structure with 2 (Ga,Mn)As layers and two NN for the structure with 3 (Ga,Mn)As layers. In the case of structure with 5

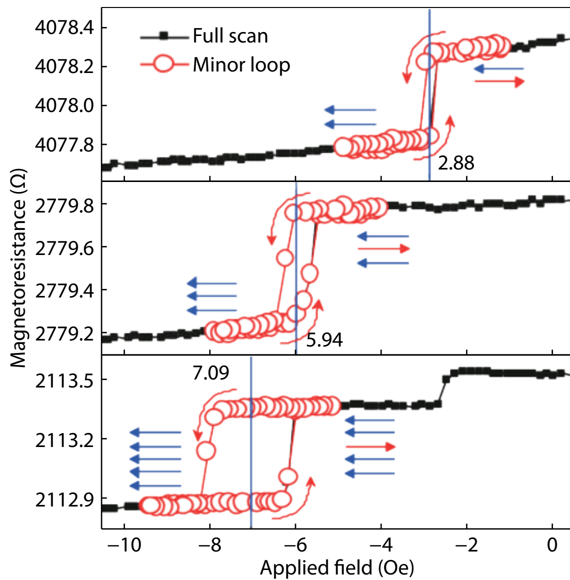


Fig. 6. (Color online) Minor MR hysteresis loops obtained during the "restoring" process for our three samples. The minor loops are plotted with red open circles on top of main loops shown by black lines. The magnetization alignments involved in the minor loop of each sample are schematically shown by arrows at corresponding values of MR. The solid vertical lines indicate minor loop shifts HMLS from zero field. (Adapted from Ref. [43])

(Ga,Mn)As layers, it has two NN and two NNN (Ga,Mn)As layers. By considering spin configurations that experienced during the minor scan, the IEC field, $H_{IEC}$, acting on the (Ga,Mn)As layer can be calculated using Eq. (1). The (Ga,Mn)As layer was counted from the top and we use the magnetization $M_i$ of $i$th layer for the calculation of the $H_{IEC}$, which can be related with the NN and NNN IEC coupling constants, $J_1$ and $J_2$, as shown in the Table 2.

The values of $H_{IEC}$ calculated using Eq. (1) for a (Ga,Mn)As layer as it experiences a magnetization reversal are listed in the second column of Table 2. These values can be compared to the experimentally observed minor loop shift $H_{MLS}$ listed in the fourth column. The values are normalized to the 2-layer sample, as listed in the third and fifth columns of Table 2, for direct comparison. The calculation shows that the $H_{IEC}$ is two times larger for the 3-layer structure than for the 2-layer structure. This is because, while the 2-layer (Ga,Mn)As structure has only one (Ga,Mn)As NN, the middle (Ga,Mn)As layer in the 3-layer structure has a (Ga,Mn)As NN layer on both sides, doubling the strength of NN IEC that acts on the center (Ga,Mn)As layer. This relation is directly observed in experiment in the form of a minor loop shift, which is indeed twice as large in the 3-layer structure as it is in the case of the 2-layer structure, as shown in the fifth column of Table 2. This clearly indicates that the strength of the NN IEC in our samples is nearly constant between any two (Ga,Mn)As layer pairs.

Table 2. Calculated IEC field $H_{IEC}$ and experimentally observed minor loop shifts $H_{MLS}$. (Adapted from Ref. [43])

| Sample | IEC field, $H_{IEC}$ | $H_{IEC}$ ratio | Minor loop shift, $H_{MLS}$ | $H_{MLS}$ ratio |
|---|---|---|---|---|
| 2-layer | $J_1 M_i$ | 1 | 2.88 | 1.00 |
| 3-layer | $2J_1 M_i$ | 2 | 5.94 | 2.06 |
| 5-layer | $(2J_1 + 2J_2)M_i$ | $2 + 2(J_2/J_1)$ | 7.09 | 2.46 |

By considering the effect of nearest neighbors, one would expect the $H_{MLS}$ ratio 2.0 in multilayer structures. However, we observed the $H_{MLS}$ ratio of 2.46 in 5-layer structure, which is clearly greater than 2.0. The increased value of 0.46, therefore, can be attributed to the contributions from the NNN IEC in the 5-layer system. This value can be expressed as $2(J_2/J_1)$ (as shown in the second column for the 5-layer structure in Table 2). The experiments directly provide a measure of the NNN IEC strength in our system as $J_2 = 0.23J_1$. This experimentally determined relative strength of NNN IEC to NN IEC, 0.23, is similar to 0.25, the value extracted by considering simply the distance separating the magnetic layers[44]. The relation between NNN IEC and NN IEC, i.e, $J_2 = 0.23J_1$, provides the value of NNN IEC field as 0.66 Oe for our (Ga,Mn)As multilayer structures.

## 4. Summary and Conclusions

We have investigated IEC phenomena in various types of (Ga,Mn)As-based multilayer structures by using magnetotransport measurements. Investigations of sample series A and B, which are different between series by Be doping in GaAs spacer, show both FM and AFM IEC depending on the structural parameters. Interestingly, AFM IEC was observed only in the Be doped samples (i.e, among series B) indicating that the presence of a carrier in the GaAs spacer is crucial for the realization of AFM IEC in the (Ga,Mn)As-based multilayer. In addition, the AFM IEC even appears in the sample with 7 nm GaAs spacer, which is much thicker than that predicted by theoretical calculation, implying that IEC in the (Ga,Mn)As-based system is quite long-ranged. Such long-ranged magnetic IEC in (Ga,Mn)As-based multilayers provided a unique opportunity for investigation of NNN IEC, which has never been reported in metallic multilayer systems. The effect of NNN IEC in (Ga,Mn)As multilayers indeed observed as interesting step-like transitions during magnetization reversal. Each transition corresponds to the flips of magnetization in specific (Ga,Mn)As layers, which feels a different magnitude of IEC owing to the influence of NNN IEC in the system. The relative strength of NNN IEC to the NN IEC in (Ga,Mn)As multilayers was experimentally determined as 0.23, which is close to the value expected from the theory.

## Acknowledgments

This research was supported by Basic Science Research Program through the National Research Foundation of Korea (NRF) funded by the Ministry of Education (2018R1D1A1A 02042965); by Ministry of Science ICT (2018R1A4A1024157); by a Korea University Future Research Grant; and by the National Science Foundation Grant DMR 1400432.

## References

[1] Binasch G, Grünberg P, Saurenbach F, et al. Enhanced magnetoresistance in layered magnetic structures with antiferromagnetic interlayer exchange. Phys Rev B, 1989, 39(7), 4828

[2] Baibich M N, Broto J M, Fert A, et al. Giant magnetoresistance of (001)Fe/(001)Cr magnetic superlattices. Phys Rev Lett, 1988, 61(21), 2472

[3] Parkin S S P, Farrow R F C, Marks R F, et al. Oscillations of interlayer exchange coupling and giant magnetoresistance in (111) oriented permalloy/Au multilayers. Phys Rev Lett, 1994, 73(8), 1190

[4] Bloemen P J H, van Kesteren H W, Swagten H J M, et al. Oscillatory interlayer exchange coupling in Co/Ru multilayers and bilayers. Phys Rev B, 1994, 50(18), 13505

[5] Borchers J A, Dura J A, Unguris J, et al. Observation of antiparallel magnetic order in weakly coupled Co/Cu multilayers. Phys Rev Lett, 1999, 82(13), 2796

[6] Parkin S S P. Systematic variation of the strength and oscillation period of indirect magnetic exchange coupling through the 3d, 4d, and 5d transition metals. Phys Rev Lett, 1991, 67(25), 3598

[7] Parkin S S P, More N, Roche K. Oscillations in exchange coupling and magnetoresistance in metallic superlattice structures: Co/Ru, Co/Cr, and Fe/Cr. Phys Rev Lett, 1990, 64(19), 2304

[8] Berger L. Emission of spin waves by a magnetic multilayer traversed by a current. Phys Rev B, 1996, 54(13), 9353

[9] Miron I M, Garello K, Gaudin G, et al. Perpendicular switching of a single ferromagnetic layer induced by in-plane current injection. Nature, 2011, 476, 189

[10] Slonczewski J C. Current-driven excitations of magnetic multilayers. J Magn Magn Mater, 1996, 159, L1

[11] Koshihara S, Oiwa A, Hirasawa M, et al. Ferromagnetic order induced by photogenerated carriers in magnetic III–V semiconductor heterostructures of (In, Mn)As/GaSb. Phys Rev Lett, 1997, 78(24), 4617

[12] Lee H, Choi S, Lee S, et al. Effect of light illumination on the [100] uniaxial magnetic anisotropy of (Ga,Mn)As film. Solid State Commun, 2014, 192, 27

[13] Lee S, Shin D Y, Chung S J, et al. Tunable quaternary states in ferromagnetic semiconductor (Ga,Mn)As single layer for memory devices. Appl Phys Lett, 2007, 90(15), 152113

[14] Liu X, Sasaki Y, Furdyna J K. Ferromagnetic resonance in $Ga_{1-x}Mn_xAs$ effects of magnetic anisotropy. Phys Rev B, 2003, 67(20), 205204

[15] Ohno H, Chiba D, Matsukura F, et al. Electric-field control of ferromagnetism. Nature, 2000, 408(6815), 944

[16] Lee H, Lee S, Choi S, et al. Interlayer exchange coupling in MBE-grown (Ga,Mn)As-based multilayer systems. J Cryst Growth, 2017, 477, 188

[17] Bac S K, Lee H, Kee S, et al. Effects on magnetic properties of (Ga,Mn)As induced by proximity of topological insulator $Bi_2Se_3$. J Electron Mater, 2018, 47(8), 4308

[18] Chang J, Bhoi S, Lee K J, et al. Effects of film thickness and annealing on the magnetic properties of (Ga,Mn)AsP ferromagnetic semiconductor. J Cryst Growth, 2019, 512, 112

[19] Yuldashev S U, Im K, Yalishev V S, et al. Effect of additional nonmagnetic acceptor doping on the resistivity peak and the Curie temperature of $Ga_{1-x}Mn_xAs$ epitaxial layers. Appl Phys Lett, 2003, 82(8), 1206

[20] Chung S, Lee S, Chung J H, et al. Giant magnetoresistance and long-range antiferromagnetic interlayer exchange coupling in (Ga,Mn)As/GaAs: Be multilayers. Phys Rev B, 2010, 82(5), 054420

[21] Chung S, Lee S, Yoo T, et al. Determination of interlayer exchange fields acting on individual (Ga,Mn)As layers in (Ga,Mn)As/GaAs multilayers. Jpn J Appl Phys, 2015, 54(3), 033001

[22] Lee H, Lee S, Choi S, et al. Antiferromagnetic interlayer exchange coupling in ferromagnetic (Ga,Mn)As/GaAs: Be multilayers. IEEE Trans Magn, 2015, 51(11), 2400604

[23] Leiner J, Lee H, Yoo T, et al. Observation of antiferromagnetic interlayer exchange coupling in a $Ga_{1-x}Mn_xAs$/GaAs: Be/$Ga_{1-x}Mn_xAs$ trilayer structure. Phys Rev B, 2010, 82(19), 195205

[24] Baxter D V, Ruzmetov D, Scherschligt J, et al. Anisotropic magnetoresistance in $Ga_{1-x}Mn_xAs$. Phys Rev B, 2002, 65(21), 212407

[25] Wang K Y, Edmonds K W, Campion R P, et al. Anisotropic magnetoresistance and magnetic anisotropy in high-quality (Ga,Mn)As films. Phys Rev B, 2005, 72(8), 085201

[26] Shin D Y, Chung S J, Lee S, et al. Temperature dependence of magnetic anisotropy in ferromagnetic (Ga,Mn)As films: Investigation by the planar Hall effect. Phys Rev B, 2007, 76(3), 035327

[27] Grünberg P A. Exchange anisotropy, interlayer exchange coupling and GMR in research and application. Sens Actuators A, 2001, 91(1), 153

[28] Giddings A D, Jungwirth T, Gallagher B L. (Ga,Mn)As based superlattices and the search for antiferromagnetic interlayer coupling. Phys Rev B, 2008, 78(16), 165312

[29] Sankowski P, Kacman P. Interlayer exchange coupling in (Ga,Mn)As-based superlattices. Phys Rev B, 2005, 71(20), 201303

[30] Szałowski K, Balcerzak T. Antiferromagnetic interlayer coupling in diluted magnetic thin films with RKKY interaction. Phys Rev B, 2009, 79(21), 214430

[31] Chung J H, Chung S J, Lee S, et al. Carrier-mediated antiferromagnetic interlayer exchange coupling in diluted magnetic semiconductor multilayers $Ga_{1-x}Mn_xAs$/GaAs:Be. Phys Rev Lett, 2008, 101(23), 237202

[32] Chung J H, Lin J, Furdyna J K, et al. Investigation of weak interlayer exchange coupling in (Ga,Mn)As/GaAs superlattices with insulating nonmagnetic spacers. J Appl Phys, 2011, 110(1), 013912

[33] Kępa H, Le V K, Brown C M, et al. Probing hole-induced ferromagnetic exchange in magnetic semiconductors by inelastic neutron scattering. Phys Rev Lett, 2003, 91(8), 087205

[34] Rhyne J J, Lin J, Furdyna J K, et al. Anomalous antiferromagnetic coupling in [ZnTe¦MnTe] superlattices. J Magn Magn Mater, 1998, 177–181, 1195

[35] Unguris J, Celotta R J, Pierce D T. Observation of two different oscillation periods in the exchange coupling of Fe/Cr/Fe(100). Phys Rev Lett, 1991, 67(1), 140

[36] Bruno P, Chappert C. Oscillatory coupling between ferromagnetic layers separated by a nonmagnetic metal spacer. Phys Rev Lett, 1991, 67(12), 1602

[37] Bruno P, Chappert C. Ruderman-Kittel theory of oscillatory interlayer exchange coupling. Phys Rev B, 1992, 46(1), 261

[38] Yafet Y. Ruderman-Kittel-Kasuya-Yosida range function of a one-dimensional free-electron gas. Phys Rev B, 1987, 36(7), 3948

[39] Chen B, Xu H, Ma C, et al. All-oxide-based synthetic antiferromagnets exhibiting layer-resolved magnetization reversal. Science, 2017, 357(6347), 191

[40] Chung S, Lee S, Yoo T, et al. The critical role of next-nearest-neighbor interlayer interaction in the magnetic behavior of magnetic/non-magnetic multilayers. New J Phys, 2013, 15(12), 123025

[41] Eid K F, Stone M B, Ku K C, et al. Exchange biasing of the ferromagnetic semiconductor $Ga_{1-x}Mn_xAs$. Appl Phys Lett, 2004, 85(9), 1556

[42] Yu K M, Walukiewicz W, Wojtowicz T, et al. Effect of film thickness on the incorporation of Mn interstitials in $Ga_{1-x}Mn_xAs$. Appl Phys Lett, 2005, 86(4), 042102

[43] Lee H, Bac S K, Lee S, et al. Experimental determination of next-nearest-neighbor interlayer exchange coupling in ferromagnetic (Ga,Mn)As/GaAs:Be multilayers. Appl Phys Lett, 2015, 107(19), 192403

[44] Han J H, Lee H W. Interlayer exchange coupling between next nearest neighbor layers. Phys Rev B, 2012, 86(17), 174426